RadioGraphics

Urinary Bladder Cancer: Role of MR Imaging[1]

Sadhna Verma, MD • Arumugam Rajesh, MBBS, FRCR • Srinivasa R. Prasad, MD • Krishnanath Gaitonde, MD • Chandana G. Lall, MD Vladimir Mouraviev, MD, PhD • Gunjan Aeron, MD • Robert B. Bracken, MD • Kumaresan Sandrasegaran, MD

ONLINE-ONLY CME

See www.rsna.org/education/rg_cme.html

LEARNING OBJECTIVES

After completing this journal-based CME activity, participants will be able to:

- List the strengths and limitations of CT and MR imaging in the diagnosis and staging of urinary bladder cancer.
- Recognize the differences between bladder cancer that invades muscle and that which does not.
- Discuss the TNM staging of bladder cancer and its effect on management decisions.

TEACHING POINTS

See last page

Urinary bladder cancer is a heterogeneous disease with a variety of pathologic features, cytogenetic characteristics, and natural histories. It is the fourth most common cancer in males and the tenth most common cancer in females. Urinary bladder cancer has a high recurrence rate, necessitating long-term surveillance after initial therapy. Early detection is important, since up to 47% of bladder cancer–related deaths may have been avoided. Conventional computed tomography (CT) and magnetic resonance (MR) imaging are only moderately accurate in the diagnosis and local staging of bladder cancer, with cystoscopy and pathologic staging remaining the standards of reference. However, the role of newer MR imaging sequences (eg, diffusion-weighted imaging) in the diagnosis and local staging of bladder cancer is still evolving. Substantial advances in MR imaging technology have made multiparametric MR imaging a feasible and reasonably accurate technique for the local staging of bladder cancer to optimize treatment. In addition, whole-body CT is the primary imaging technique for the detection of metastases in bladder cancer patients, especially those with disease that invades muscle.

Introduction

Bladder cancer is one of the most common malignancies of the urinary tract, with an estimated 70,530 new cases per year and accounting for 14,680 cancer-related deaths in the United States in 2010 (1). It is the fourth most common cancer in males and the tenth most common cancer in females. Urinary bladder cancer occurs three to four times more frequently in men than in women (1) and has a high recurrence rate, necessitating long-term surveillance after initial therapy. Patients with bladder cancer survive longer than those with most other common cancers. As a result, the lifetime costs of treatment and follow-up have been estimated at $100,000–$120,000 (2). It is also estimated that the 5-year cost of treating Medicare patients with this pathologic condition is about $1 billion, seventh highest among all cancers (3).

Abbreviations: ADC = apparent diffusion coefficient, FIESTA = fast imaging employing steady-state acquisition, FOV = field of view, GRE = gradient-echo, SE = spin-echo, 3D = three-dimensional, TURBT = transurethral resection of bladder tumor

RadioGraphics 2012; 32:371–387 • **Published online** 10.1148/rg.322115125 • **Content Codes:** GU MR OI

[1]From the Departments of Radiology (S.V., G.A.) and Urology (K.G., V.M., R.B.B.), University of Cincinnati Medical Center, 234 Goodman St, PO Box 670761, Cincinnati, OH 45267-0761; Department of Radiology, University Hospitals of Leicester NHS Trust, Leicester, England (A.R.); Department of Radiology, M. D. Anderson Cancer Research Center, Houston, Tex (S.R.P.); Department of Radiology, University of California–Irvine, Orange, Calif (C.G.L.); and Department of Radiology, Indiana University School of Medicine, Indianapolis, Ind (K.S.). Presented as an education exhibit at the 2010 RSNA Annual Meeting. Received May 31, 2011; revision requested July 8 and received November 14; accepted November 16. For this journal-based CME activity, author K.S. has disclosed various financial relationships (see p 384); all other authors, the editor, and reviewers have no relevant relationships to disclose. **Address correspondence to** S.V. (e-mail: *drsadhnaverma@gmail.com*).

In this article, we discuss urinary bladder cancer in terms of pathologic features, genetic characteristics, clinical staging and management, treatment, and imaging considerations, with emphasis on the value of conventional and newer imaging techniques for diagnosis and local staging.

Pathologic Features

Teaching Point

About 90% of bladder tumors are urothelial in origin (ie, transitional cell carcinomas). Squamous cell carcinomas account for 6%–8% of all bladder cancers (4,5). Adenocarcinomas are rare and typically represent urachal cancer. Up to 25% of urothelial cancers have a mixed histology that includes small cell neuroendocrine, micropapillary (resembling serous papillary cancer of the ovary), sarcomatoid, and plasmacytoid components. These variants have substantially worse prognoses than do the pure urothelial cancers. The most common etiologic factors for urothelial tumors are cigarette smoking and occupational exposure to chemical carcinogens such as aniline dyes (6,7). Cigarette smoking is thought to be the causative factor in 50%–60% of men and one-third of women who develop bladder cancer (8,9). The relative risk of current smokers for death from bladder cancer is 3.3 in men and 2.2 in women. Iatrogenic risk factors for urothelial tumors are therapeutic irradiation of neighboring organs and the use of alkylating agents. Although it is rare, there is a genetic predisposition to the development of urothelial tumors in some families (10,11). Risk factors for squamous cell cancer include long-term catheterization, nonfunctioning bladder, urinary tract calculi, and chronic infection by *Schistosoma hematobium*.

Teaching Point

Urothelial tumors are classified as either invading muscle (nonpapillary) or not invading muscle (superficial or papillary). Approximately 80%–85% of urothelial tumors are non–muscle invasive. These are low-grade lesions, can be multifocal, and arise from a hyperplastic epithelium. They generally have a good prognosis and rarely evolve into an invasive cancer, although urothelial recurrence rates are about 50% (12,13). Approximately 20%–25% of bladder cancers are muscle invasive, arise from severe dysplasia or carcinoma in situ, and have a higher histologic grade (14). Non-muscle-invasive urothelial tumors have a higher rate of recurrence than do the muscle-invasive variety. If left untreated, they are a precursor of muscle-invasive tumors. Nearly all cases of squamous carcinoma and adenocarcinoma of the bladder are invasive at the time of diagnosis. These two types of bladder cancer can carry a worse prognosis than do urothelial tumors, even with aggressive surgical therapy and chemotherapy.

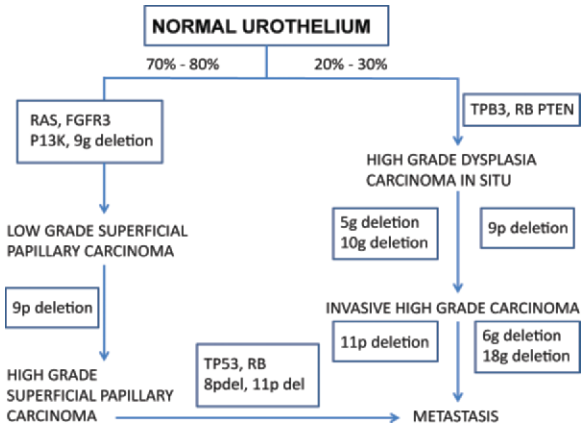

Figure 1. Chart illustrates the molecular biology of muscle-invasive and non-muscle-invasive papillary tumors.

Genetic Characteristics

Non-muscle-invasive and muscle-invasive tumors behave differently because they harbor distinctive genetic defects and arise along two separate pathways (Fig 1). Non-muscle-invasive tumors are characterized by activating mutations in the HRAS gene and fibroblast growth factor. These genes play a role in modulating the RTK (receptor tyrosine kinase)/RAS signaling pathway. Activation of the RTK/RAS pathway leads to the development of malignancy. Patients with non-muscle-invasive tumors may benefit from RTK/RAS pathway inhibition.

Muscle-invasive tumors are characterized by structural and functional defects in the p53 and retinoblastoma tumor suppressor pathways. Both of these proteins play critical roles in cell cycle control (15,16). These high-grade tumor variants tend to metastasize despite radical surgery, but affected patients could potentially benefit from replacement therapies that restore the functions of p53 and retinoblastoma.

On the basis of the molecular pathogenesis of bladder cancer, several U.S. Food and Drug Administration–approved biomarkers are available for predicting disease recurrence and survival after radical cystectomy (17). To date, however, none of the approved biomarker assays eliminate the need for diagnostic or surveillance cystoscopy (18).

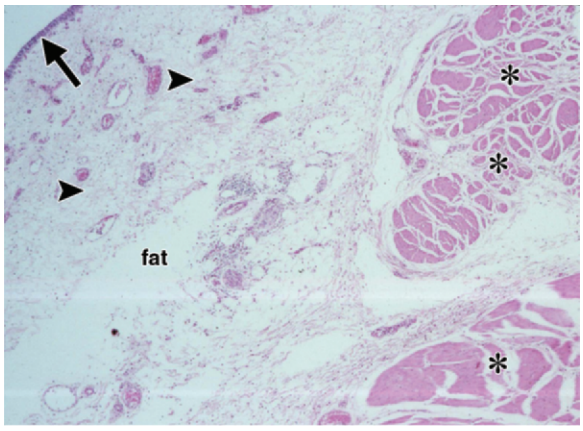

a.

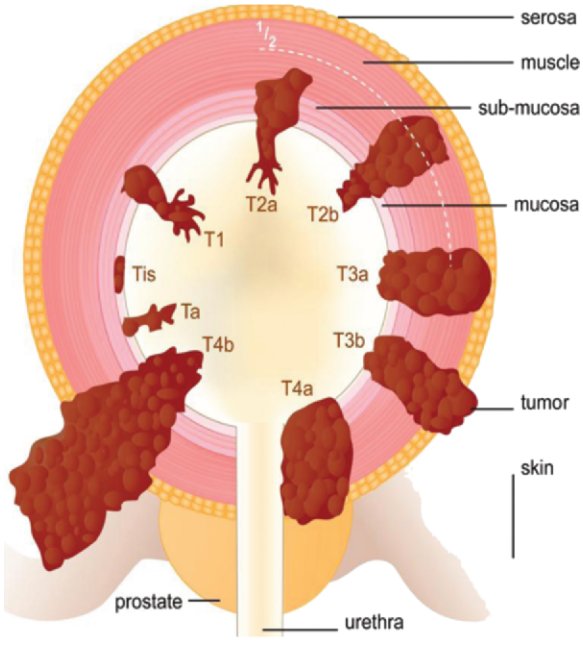

b.

Figure 2. **(a)** Photomicrograph (original magnification, ×20; hematoxylin-eosin stain) of the normal bladder wall shows the urothelium (arrow), submucosa (arrowheads), and detrusor muscle (*). **(b)** Drawing illustrates the layers of the bladder wall and tumor staging based on depth of invasion. (See Table for T stage definitions.)

Normal Anatomy of the Urinary Bladder

The urinary bladder is primarily an extraperitoneal structure, with peritoneum covering only the superior surface of the bladder (bladder dome). The orifices of the ureters at the ureterovesical junction are joined by an elevated ridge covered by mucosa (the interureteric ridge). The bladder trigone is a triangular region on the inferior wall, marked at its corners by the ureterovesical junction and the urethra. The four defined layers of the bladder wall are *(a)* the urothelium, which lines the bladder lumen; *(b)* the highly vascular lamina propria (submucosa); *(c)* the muscularis propria; and *(d)* the outermost serosa (Fig 2a) (6,19). The urothelium is thin relative to the full thickness of the bladder wall. The thickness of the highly vascular lamina propria varies with the degree of distention of the bladder. The muscular layer of the bladder is also referred to as the detrusor muscle and consists of a complex network of interlacing smooth muscle fibers. The inner and outer muscle fibers tend to be oriented in a longitudinal fashion, but distinct layers are usually not discernible. The outermost serosa is formed by a loose layer of connective tissue.

Clinical Staging and Management

Patients with bladder cancer most commonly present with painless hematuria (80%–90% of cases) (6). The initial evaluation of a patient who presents with hematuria is not uniform: Some institutions perform computed tomographic (CT) urography for triage prior to cystoscopy, whereas others use cystoscopy as the first line of investigation. Nevertheless, cystoscopy and CT are complementary and have a definite management role in patients who present with hematuria. Magnetic resonance (MR) imaging of the pelvis is usually performed for T (tumor) staging once bladder cancer has been diagnosed, although its use is not widespread.

Cystoscopic staging to evaluate the urinary bladder and urethral mucosa is an important part of pretreatment planning. Cystoscopic biopsy of suspicious-looking bladder lesions is performed to assess the pathology, grade, and depth of these tumors. Transurethral resection of bladder tumor (TURBT) is performed for complete resection of superficial bladder tumors. TURBT is also used for deep biopsy to assess for muscle-invasive tumors. Cross-sectional imaging is usually performed afterward for disease staging in patients who are thought to have solid tumors. Treatment decisions and prognosis for bladder cancer are based on the depth of muscle invasion by the tumor, degree of differentiation of the tumor, and presence or absence of metastatic disease. Ureteroscopy is performed in patients with positive selective ureteral cytologic findings or evidence of upper tract disease at CT urography. Biopsy is performed of all suspicious-looking lesions.

TNM Guidelines for the Staging of Urinary Bladder Cancer

Descriptor	Definition
Tumor	
Tx	Primary tumor cannot be evaluated
T0	No primary tumor
Ta	Noninvasive papillary carcinoma
Tis	Carcinoma in situ
T1	Tumor invades connective tissue under the epithelium (surface layer)
T2	Tumor invades muscle
T2a	Superficial muscle affected (inner half)
T2b	Deep muscle affected (outer half)
T3	Tumor invades perivesical fat
T3a	Tumor is detected microscopically
T3b	Extravesical tumor is visible macroscopically
T4	Tumor invades the prostate gland, uterus, vagina, pelvic wall, or abdominal wall
Node	
Nx	Regional lymph nodes cannot be evaluated
N0	No regional lymph node metastasis
N1	Metastasis in a single lymph node <2 cm in size
N2	Metastasis in a single lymph node >2 cm but <5 cm in size, or multiple lymph nodes <5 cm in size
N3	Metastasis in a lymph node >5 cm in size
Metastasis	
Mx	Distant metastasis cannot be evaluated
M0	No distant metastasis
M1	Distant metastasis

Source.—Reference 20.

Bladder cancer is staged using the TNM (tumor-node-metastasis) staging system (Table) (20). In this system, T stage is based on the degree of invasion of the bladder wall (Fig 2b). TURBT is usually chosen as the initial treatment for early-stage urinary bladder carcinoma. Tumors of stage T2 or greater are treated with partial or total cystectomy or with adjuvant therapies, since TURBT for invasive tumors often results in local tumor recurrence. Therefore, preoperative differentiation between stage T1 tumors and stage T2 (or greater) tumors is crucial for the appropriate choice of effective treatment options.

Treatment

Non-Muscle-invasive Disease

Non-muscle-invasive tumors are usually treated with TURBT. Despite being the primary staging technique, clinical staging understages 30%–50% of bladder cancers (21–23). As a result, in patients with bulky Ta lesions or T1 tumors, the current trend is to perform repeat TURBT 2–6 weeks after the first TURBT. At repeat TURBT, residual disease is seen in one-third to three-fourths of patients. At many centers, lesions that carry an increased risk of recurrence are treated with adjuvant intravesical chemotherapy (eg, with mitomycin C or gemcitabine) or immunotherapy (with bacille Calmette-Guérin [BCG]). Although response rates are about 80%, 70% of patients with non-muscle-invasive bladder cancer develop recurrences within 3 years of treatment, 10%–20% of which are invasive (24).

Muscle-invasive Disease

For muscle-invasive tumors, radical cystectomy is the established treatment. The 5-year survival rate for patients who have undergone cystectomy varies from 27% for stage T4 disease to 66% for stage T2 disease. There is evidence that the extent of lymphadenectomy correlates with survival,

with meticulous lymphadenectomy resulting in a 30% cure rate for node-positive cancer. The concept of the sentinel node is not generally accepted for bladder cancer; thus, extended bilateral lymphadenectomy is required. Robotic cystectomy is increasingly being practiced, although long-term oncologic outcomes following this surgical technique are not yet available. Up to 50% of patients with muscle-invasive bladder cancer eventually develop metastatic disease (25).

Imaging Considerations

Computed Tomography

CT urography has a sensitivity and specificity of over 90% for the diagnosis of bladder cancer in patients with hematuria (26). In patients who are at low risk for cancer, such as those less than 40 years of age or female nonsmokers, CT urography may be sufficient for detecting the presence of bladder cancer. Despite these encouraging results, CT urography cannot be used as a replacement for diagnostic cystoscopy in most patients with suspected bladder cancer. CT does not typically allow the confident diagnosis of flat lesions and lesions at the bladder base adjacent to the prostate gland, particularly in patients with benign prostatic hypertrophy. A major difficulty is differentiating tumor recurrence from inflammatory wall thickening that occurs following endovesical chemotherapy, and from scar tissue after TURBT.

The general techniques for CT urography have been previously published (27,28). The homogeneous opacification of urine has been claimed to improve bladder cancer detection, particularly on the nondependent surface of the bladder. Specialized techniques have been suggested, such as having patients void prior to CT and then administering intravenous diuretics to increase bladder filling (13,29,30).

It is possible to visualize bladder wall enhancement and thickness on nephrographic phase CT scans. Virtual cystoscopy has been performed with the installation of 300–500 mL of air or carbon dioxide into the bladder lumen via a catheter (31). Although some small series have shown CT cystoscopy to have a sensitivity of over 90%, it is probable that any additional diagnostic sensitivity is outweighed by *(a)* the invasiveness of the procedure; *(b)* the fact that cystoscopy is required for the detection of small flat lesions; and *(c)* the reduced sensitivity of virtual cystoscopy for dependent lesions, where there may be a pool of urine obscuring the mucosa.

MR Imaging

The study of the bladder requires high spatial resolution, which can be achieved with the use of a phased-array external surface coil (such as a cardiac coil), thin sections (3 mm), and a large matrix (32). Use of a rectangular field of view (FOV) helps reduce imaging time, but care should be taken to avoid extensive aliasing, which is usually reduced by applying presaturation pulses in the phase-encoding direction within the FOV.

Preliminary localizer sequences are used to evaluate for appropriate coil placement and bladder distention. A 28- to 32-cm axial FOV is usually sufficient to evaluate the bladder and surrounding soft-tissue structures (33). Optimizing echo time (usually 60–80 msec) is crucial for achieving a high contrast-to-noise ratio, which is important in assessing the depth of bladder wall involvement.

Significant artifacts in bladder imaging include lack of bladder distention, motion artifact, and chemical shift artifact. Lack of bladder distention may limit the detection of small tumors secondary to detrusor muscle thickening. On the other hand, overdistention of the bladder may result in patient motion and can decrease sensitivity for plaquelike lesions. Optimal bladder distention is achieved by instructing the patient to void approximately 2 hours prior to imaging (34). Artifact from bowel peristalsis, which can propagate from the abdomen into the pelvis, can be minimized by administering an intramuscular antiperistaltic agent and using anterior saturation bands. Motion correction on the imagers can reduce motion artifact in the area of interest by swapping phase and frequency. Chemical shift artifact refers to misregistration of spatial information caused by the difference in the resonant frequencies of water and fat. This artifact is evident only in the frequency-encoding (readout) direction and occurs at a water-fat interface (35). Typically, chemical shift manifests as high- and low-signal-intensity bands along a water-fat interface perpendicular to the frequency-encoding direction (35). This difference in frequency directly relates to the main magnetic field. The frequency difference between fat and water is 220 Hz at 1.5 T and 440 Hz at 3.0 T. At a fixed bandwidth, the pixel width of the bandlike artifact widens as field strength increases, which can limit the visualization of disease, particularly around the bladder wall. This artifact appears as a thickened

Figure 3. Papillary urothelial carcinoma (stage Ta) in a 76-year-old man. **(a)** On a CT scan obtained with a split-bolus injection of contrast material to acquire dynamic enhanced and urographic phase images, one can barely make out the presence of a tumor. It is not possible to differentiate the tumor from the detrusor muscle. **(b)** Axial high-resolution T2-weighted MR image shows multifocal bladder tumors (black arrowheads). Note the chemical shift artifact, which appears as a thickened dark line along the lateral bladder wall (detrusor muscle) (arrow) and as a nearly imperceptible thin bright line on the contralateral side (white arrowheads). **(c)** On an axial three-dimensional (3D) spoiled gradient-echo (GRE) image obtained 20 seconds after contrast material injection, the multifocal bladder tumors show intense enhancement (arrowheads), unlike the muscle layer (arrow). **(d)** Axial 3D spoiled GRE image obtained 60 seconds after contrast material administration shows delayed enhancement of the muscle layer (arrow). Arrowheads = tumors.

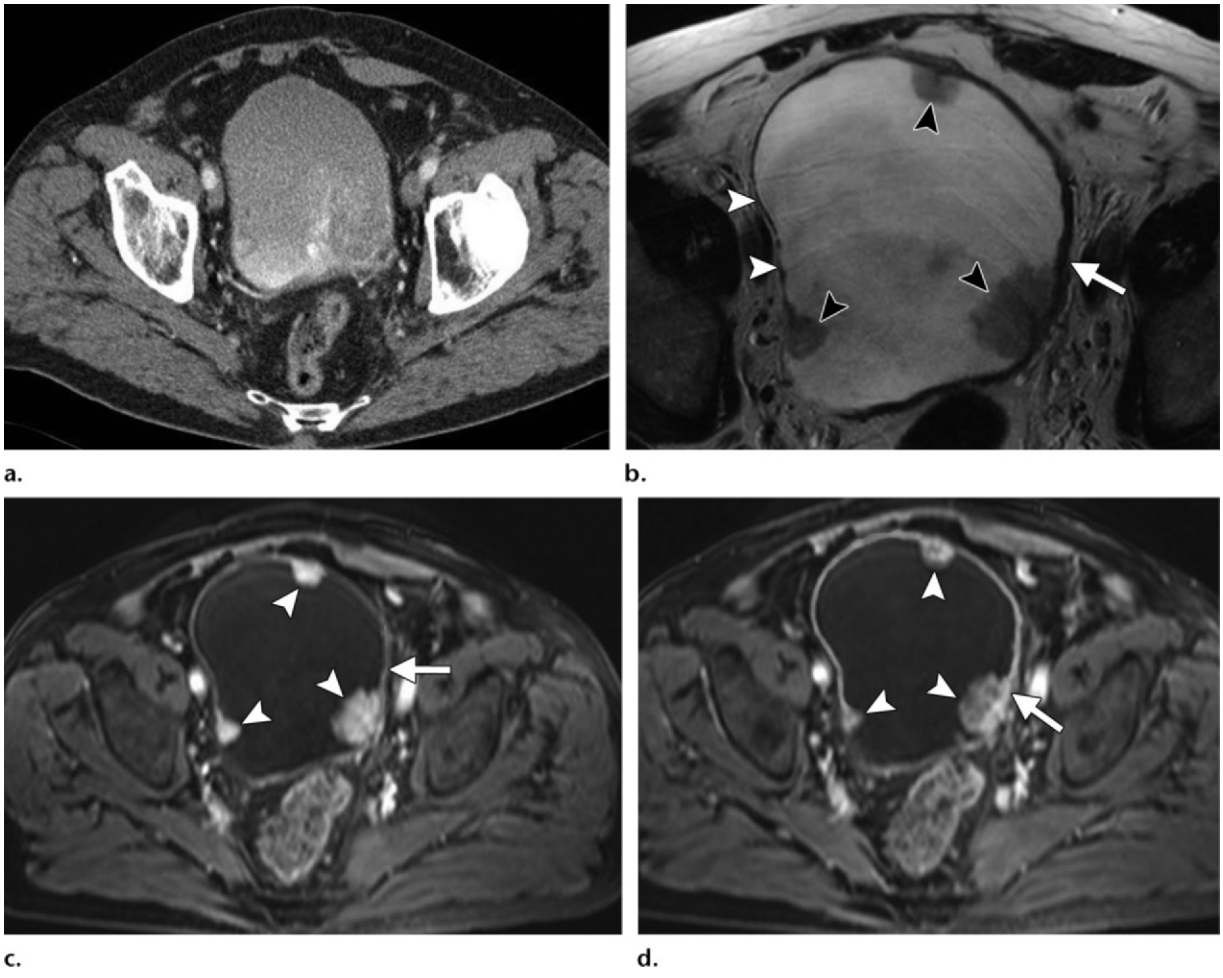

dark line along the lateral bladder wall on one side and as a bright line on the contralateral side (Fig 3b). To reduce this artifact, the bandwidth must be increased and the frequency-encoding gradient changed to select the direction that least interferes with examination of the bladder wall adjacent to the tumor (33).

MR imaging has been shown to allow more accurate staging of bladder carcinomas than CT because of its high soft-tissue contrast resolution, which allows clear differentiation between bladder wall layers (36). MR imaging has also been shown to better depict intramural tumor invasion as well as extravesical extension and allows differentiation between muscle-invasive and non-muscle-invasive disease. In addition, MR imaging has the advantage of involving no ionizing radiation.

Teaching Point

Currently, for local staging of bladder cancer, a multiparametric approach with conventional and functional sequences is useful. Axial spin-echo (SE) T1-weighted images with a large FOV are useful for evaluating the perivesical fat planes for extravesical tumor infiltration, pelvic lymphadenopathy, and bone metastases. The urine in the bladder has low signal intensity on T1-weighted images, whereas the bladder wall has intermediate signal intensity and the adjacent fat has high signal intensity. On T2-weighted images, the urine has high signal intensity and the bladder wall has low signal intensity. Non-fat-satu-

Figure 4. Urothelial carcinoma (stage T2) in a 74-year-old man. **(a)** CT scan obtained with a split-bolus injection of contrast material to acquire dynamic enhanced and urographic phase imaging data shows a tumor (*) on the right lateral bladder wall. It is not possible to differentiate the tumor from the detrusor muscle. **(b)** Axial high-resolution T2-weighted MR image shows the tumor (*). Arrow = normal low-signal-intensity detrusor muscle, arrowhead = interruption of the detrusor muscle by the tumor in keeping with stage T2 disease. **(c)** Axial 3D spoiled GRE image obtained 20 seconds after contrast material administration shows the tumor (*), which has enhanced earlier than the muscle layer (arrow). **(d)** On an axial 3D spoiled GRE image obtained 60 seconds after contrast material administration, the detrusor muscle shows delayed enhancement (arrow), as well as interruption (arrowhead) by the tumor (*), findings that are consistent with stage T2 disease. **(e)** Photomicrograph (original magnification, ×20; hematoxylin-eosin stain) shows stage T2 tumor (double arrow) with invasion of the detrusor muscle (single arrow).

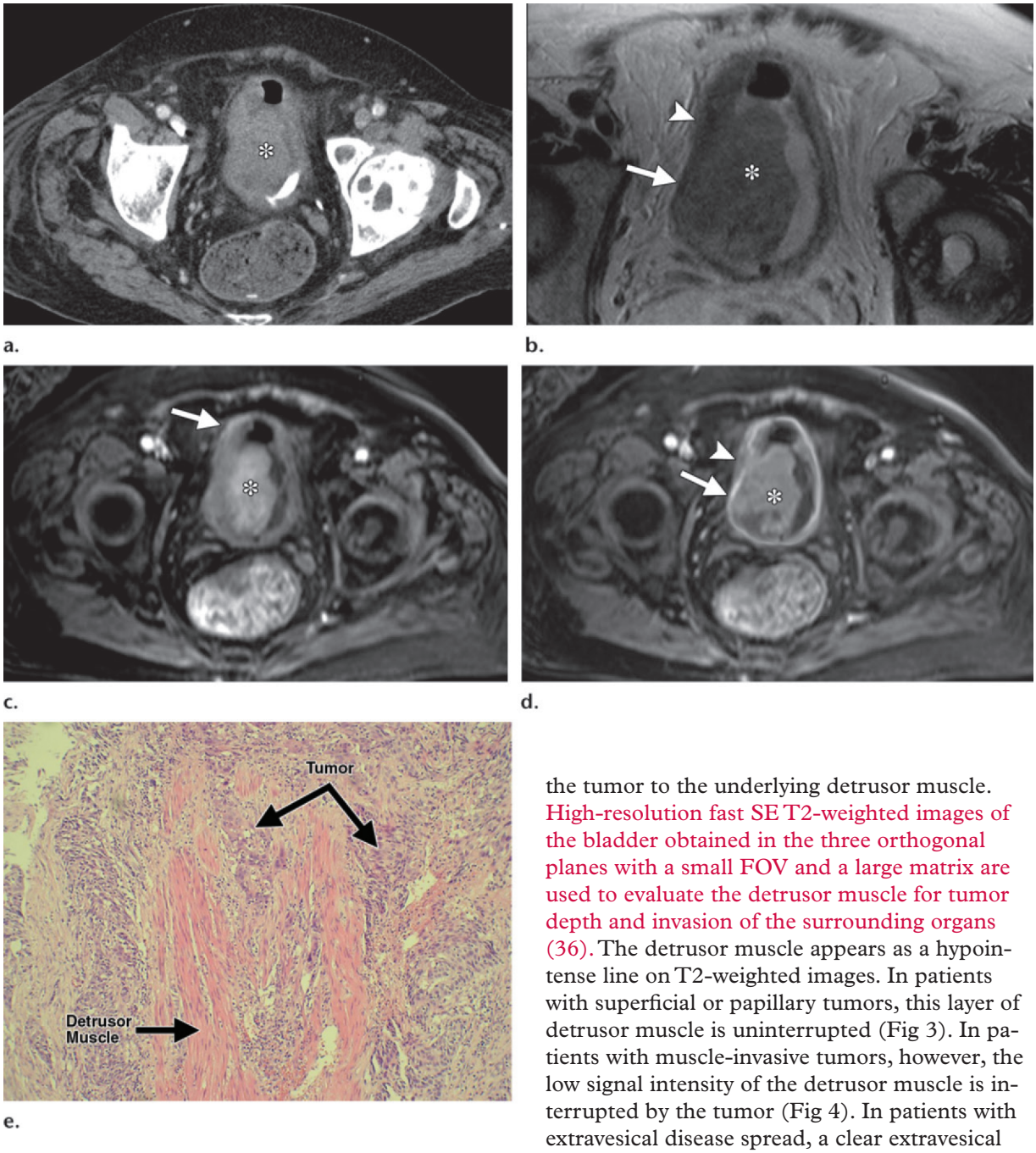

rated fast SE T2-weighted images are obtained in the three standard orthogonal planes. The plane of acquisition perpendicular to the bladder mass allows optimal depiction of the relationship of the tumor to the underlying detrusor muscle. High-resolution fast SE T2-weighted images of the bladder obtained in the three orthogonal planes with a small FOV and a large matrix are used to evaluate the detrusor muscle for tumor depth and invasion of the surrounding organs (36). The detrusor muscle appears as a hypointense line on T2-weighted images. In patients with superficial or papillary tumors, this layer of detrusor muscle is uninterrupted (Fig 3). In patients with muscle-invasive tumors, however, the low signal intensity of the detrusor muscle is interrupted by the tumor (Fig 4). In patients with extravesical disease spread, a clear extravesical mass can be seen in stage T3b disease (Fig 5), and adjacent organ invasion can also be visualized in stage T4 disease (Fig 6).

Teaching Point

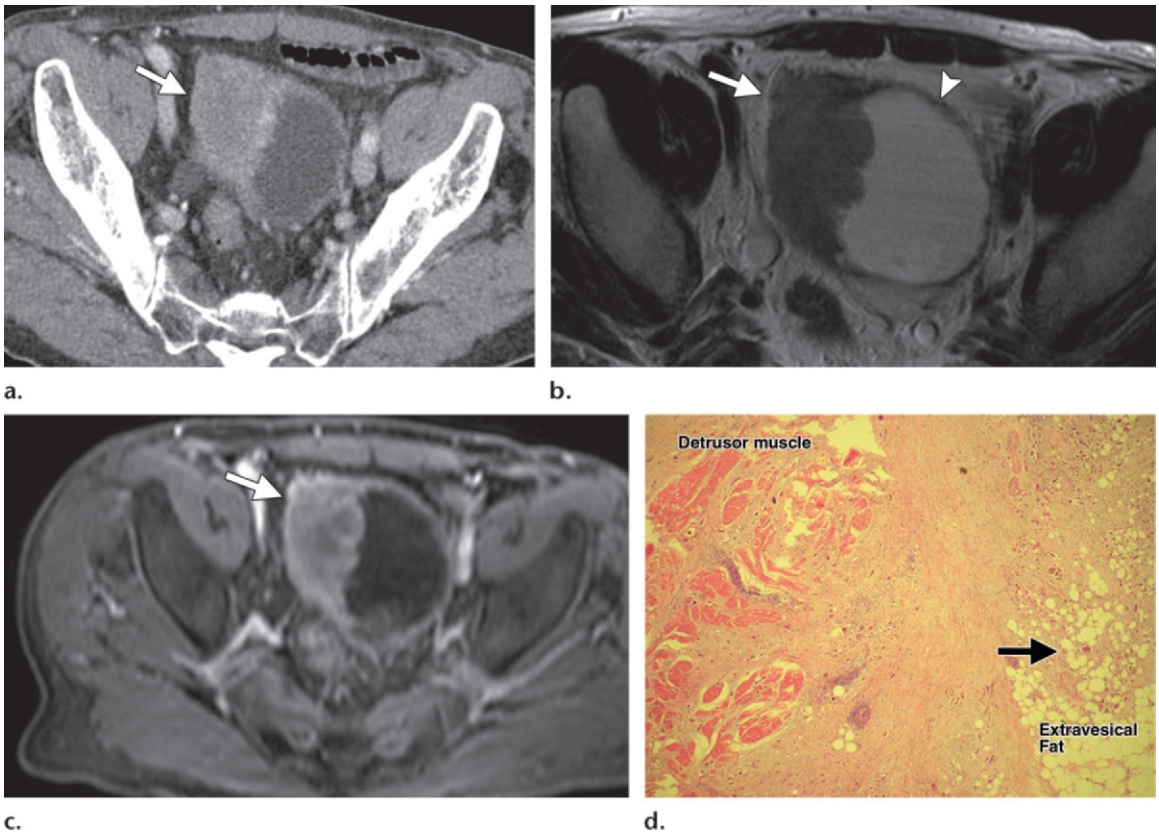

Figure 5. Urothelial carcinoma (stage T3b) in an 84-year-old man. **(a)** CT scan obtained with a split-bolus injection of contrast material to acquire dynamic enhanced and urographic phase imaging data shows extravesical tumor spread (arrow). **(b)** Axial high-resolution T2-weighted MR image shows a bladder tumor. Arrow = extravesical mass in keeping with stage T3b disease, arrowhead = normal detrusor muscle. **(c)** Axial 3D spoiled GRE image obtained 60 seconds after contrast material administration shows the extravesical mass (arrow). **(d)** Photomicrograph (original magnification, ×40; hematoxylin-eosin stain) shows stage T3 tumor with extension (arrow) into the extravesical fat.

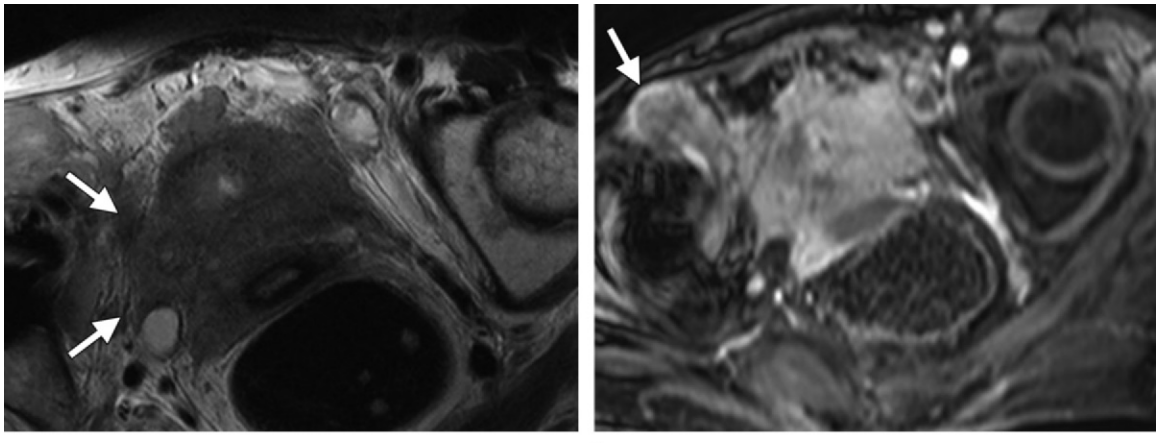

Figure 6. Urothelial carcinoma (stage T4) in an 80-year-old woman. Axial high-resolution T2-weighted MR image **(a)** and 3D spoiled GRE image obtained 60 seconds after contrast material administration **(b)** show an extravesical mass (arrows) involving the pelvic wall and cervix. TURBT initially showed stage T2 disease, but deeper follow-up biopsy helped confirm stage T4 disease.

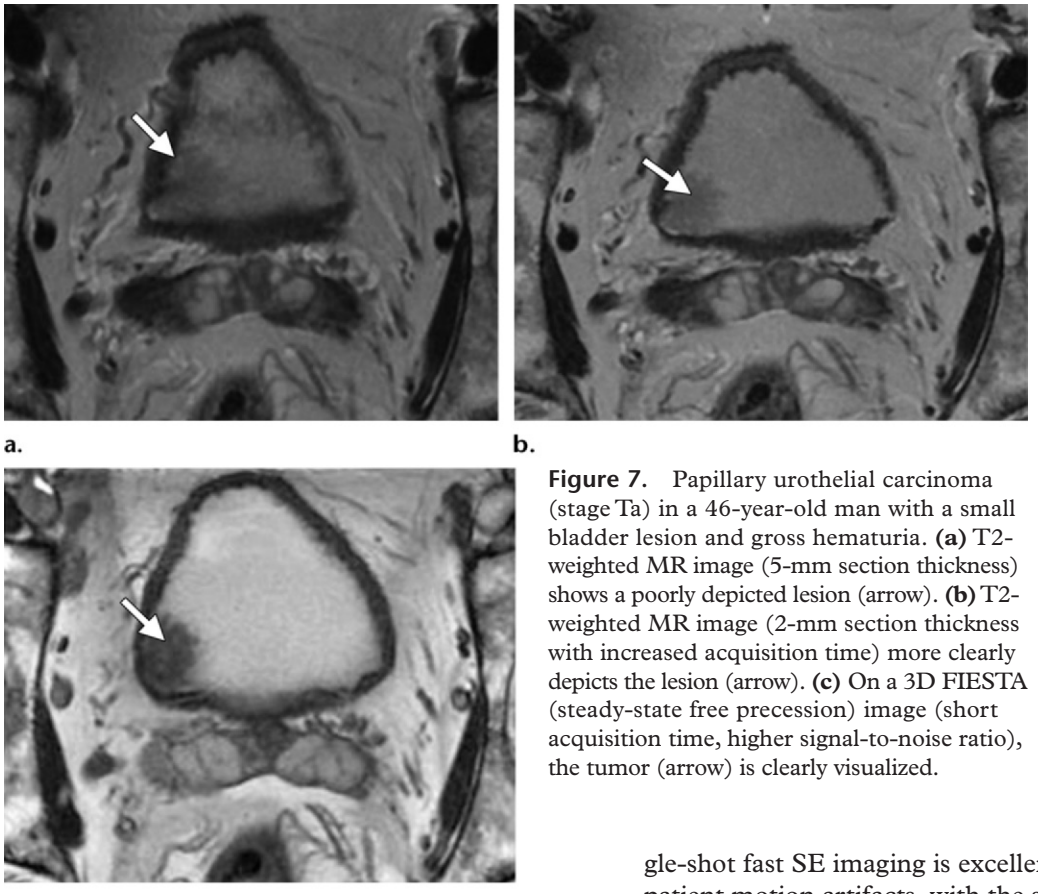

Figure 7. Papillary urothelial carcinoma (stage Ta) in a 46-year-old man with a small bladder lesion and gross hematuria. **(a)** T2-weighted MR image (5-mm section thickness) shows a poorly depicted lesion (arrow). **(b)** T2-weighted MR image (2-mm section thickness with increased acquisition time) more clearly depicts the lesion (arrow). **(c)** On a 3D FIESTA (steady-state free precession) image (short acquisition time, higher signal-to-noise ratio), the tumor (arrow) is clearly visualized.

The multiplanar capability of MR imaging allows image acquisition in different planes to minimize partial volume averaging and optimize imaging when evaluating the depth of bladder wall invasion. Coronal images are useful for delineating tumors located in the lateral bladder wall and dome, whereas sagittal images better depict lesions of the anterior and posterior wall and dome.

Recent advances in MR imaging technology have made 3D imaging feasible. Relative to two-dimensional sequences, 3D sequences offer the advantages of shorter acquisition time, volumetric coverage without intersection gaps, and an improved signal-to-noise ratio (Fig 7) (33). Techniques that are useful in rapid pelvic imaging include non-breath-hold ultrafast SE T2-weighted sequences (eg, single-shot fast SE and GRE sequences) and steady-state free precession imaging sequences (eg, fast imaging employing steady-state acquisition [FIESTA]) (Fig 7c). Single-shot fast SE imaging is excellent for reducing patient motion artifacts, with the same spatial resolution as conventional T2-weighted imaging but with a slightly reduced signal-to-noise ratio. The FIESTA sequence offers a very high signal-to-noise ratio, but patient motion is a problem with this sequence.

Dynamic Contrast Material–enhanced MR Imaging.—The usefulness of dynamic contrast-enhanced T1-weighted MR imaging is debatable, with some studies showing that it is a useful technique and others showing that it is of no additional value (31,37).

Three-dimensional fat-suppressed fast spoiled GRE T1-weighted images are obtained before and after contrast material administration. Three-dimensional acquisition allows multiplanar reformation. The normal bladder wall does not enhance avidly on the early gadolinium-enhanced images, which becomes important in tumor imaging. In the early phase (20 seconds after contrast material injection), bladder carcinomas tend

Figure 8. Urothelial carcinoma (stage T1) in a 58-year-old man. **(a)** CT scan obtained with a split-bolus injection of contrast material to acquire dynamic enhanced and urographic phase imaging data shows a tumor (arrow) close to the left ureteric orifice. It is not possible to differentiate the tumor from the detrusor muscle. **(b)** Axial high-resolution T2-weighted MR image shows the tumor (black arrowhead). Note the chemical shift artifact, which appears as a thickened dark line along the lateral bladder wall on one side (arrow) and as a nearly imperceptible thin bright line on the contralateral side (white arrowheads) (cf Fig 3b). **(c)** On an axial 3D spoiled GRE image obtained 20 seconds after contrast material administration, the tumor (arrowhead) has enhanced earlier than the muscle layer (arrow). **(d)** Axial 3D spoiled GRE image obtained 60 seconds after contrast material administration shows delayed enhancement of muscle (arrow) and decreased tumor enhancement (arrowhead). **(e)** Photomicrograph (original magnification, ×100; hematoxylin-eosin stain) shows stage T1 tumor with early lamina propria invasion (arrows) but no deep muscle invasion.

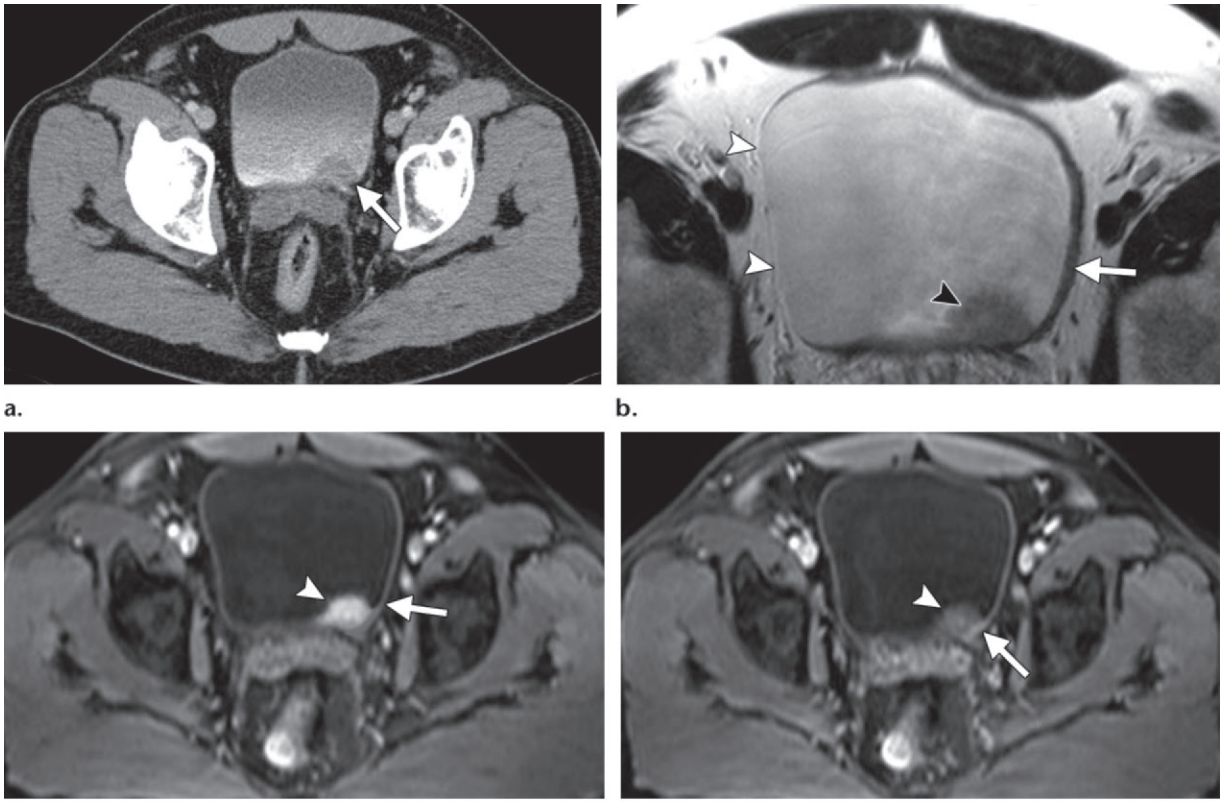

Teaching Point

to enhance more than the surrounding bladder wall (38). The bladder tumor, mucosa, and submucosa enhance early, but the muscle layer maintains its hypointensity and enhances late (60 sec) (Figs 3, 4, 8) (36). This early phase of contrast enhancement also helps distinguish the bladder tumor from the low-signal-intensity urine. On delayed (>5 min) postcontrast T1-weighted images, urine has high signal intensity and the intraluminal portion of the bladder tumor is clearly depicted, although small bladder wall tumors are obscured.

Diffusion-weighted MR Imaging.—Diffusion-weighted MR imaging is increasingly being used for cancer assessment throughout the body and has shown great promise in the detection and characterization of other genitourinary malignancies (37,39–44). The role of diffusion-weighted imaging in bladder cancer is evolving and has not yet been fully established. Diffusion-weighted

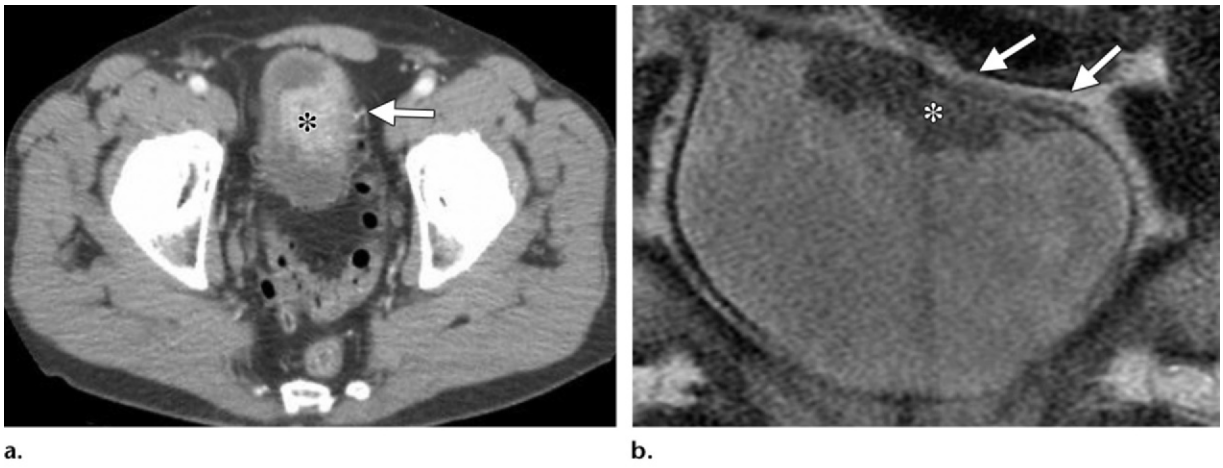

a. b.

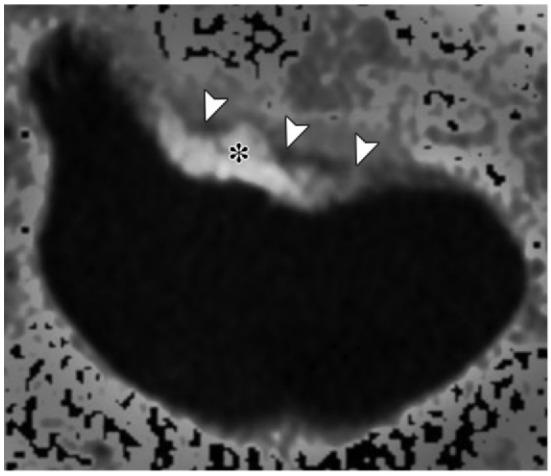

c.

Figure 9. Urothelial carcinoma (stage T2b) in a 63-year-old man. **(a)** Contrast-enhanced CT scan shows a 3.5-cm mass (*) along the bladder dome with possible perivesical extension (arrow). **(b)** Coronal T2-weighted MR image shows an irregular hypointense mass (*) along the bladder dome. It is difficult to evaluate for perivesical extension (arrows). **(c)** Coronal exponential ADC diffusion-weighted image shows bladder wall involvement by the high-signal-intensity tumor (*). There is no perivesical extension (arrowheads). Results of partial cystectomy confirmed stage T2b disease.

imaging provides both qualitative and quantitative information that reflects changes at the cellular level concerning tumor cellularity and cell membrane integrity. For most bladder tumors, increased cellular density manifests as increased signal intensity on diffusion-weighted images with a reduced apparent diffusion coefficient (ADC) at quantitative analysis (45). At some institutions, diffusion-weighted imaging is currently being used primarily for local staging (Fig 9). A single-shot SE echoplanar sequence performed with chemical shift–selective fat-suppression techniques at *b* values of 0 and 1000 sec/mm^2 is used. Diffusion gradients are applied in the three orthogonal directions, and images are obtained in the axial and sagittal planes. These images are usually evaluated together with the T2-weighted images. Initial results in the evaluation of diffusion-weighted images demonstrated reduced ADC in bladder cancer ($1.18 \pm 0.19 \times 10^{-3}$ mm^2/sec) compared with the normal bladder wall ($2.27 \pm 0.24 \times 10^{-3}$ mm^2/sec) (46). There is substantial interobserver variation in ADC values obtained in regions of interest in a relatively thin bladder wall. Therefore, changes in signal intensity seen on diffusion-weighted images are more useful than information from ADC measurements (47). Diffusion-weighted imaging in bladder cancer has been evaluated in terms of diagnosis, staging, prediction of histologic grade, and assessment of the efficacy of induction chemotherapy (46,48–52). It has shown improved differentiation between the tumor, muscle layer, and thickened submucosa, all of which have different signal intensities at diffusion-weighted imaging.

Positron Emission Tomography

Positron emission tomography (PET) with 2-[fluorine-18]fluoro-2-deoxy-D-glucose is considered to be of lesser value in the local staging of bladder cancer due to urinary excretion of the radiotracer. A study of 55 patients with bladder cancer that was performed to evaluate the usefulness of PET/CT in preoperatively diagnosing metastatic disease found a sensitivity, specificity, positive predictive value, and negative predictive value of 60%, 88%, 75%, and 79%, respectively (53). Another prospective study of 43 patients with muscle-invasive bladder cancer reported that PET/CT had a sensitivity, specificity, positive-predictive value, and negative-predictive value of 70%, 94%, 78%, and 91%, respectively (54).

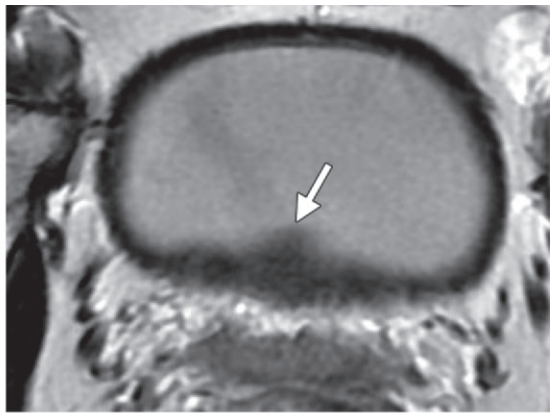

a.

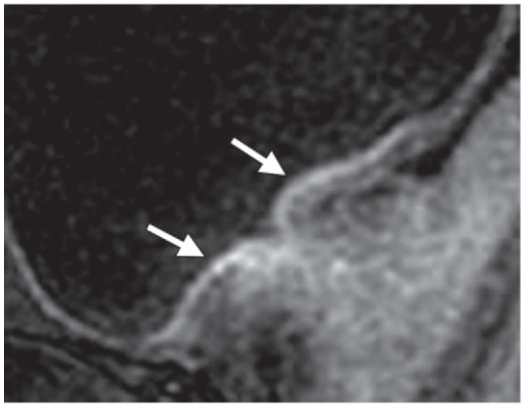

b.

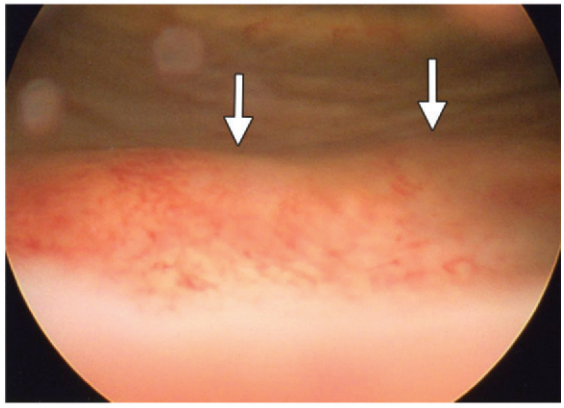

c.

Figure 10. Follow-up imaging in a 50-year-old man who had previously undergone treatment for low-grade urothelial carcinoma. **(a)** Axial T2-weighted MR image shows focal thickening at the bladder base (arrow), a finding that suggests recurrence. **(b)** Sagittal diffusion-weighted image depicts the interureteric ridge as a slightly elevated smooth surface (arrows). **(c)** Cystoscopic image shows a normal interureteric ridge (arrows) and no malignancy.

PET is not used for staging bladder cancer at our institutions. Radiotracers such as carbon-11 (^{11}C) methionine or ^{11}C choline are not excreted in urine and may be of more use as PET agents, but they have not yet been approved by the U.S. Food and Drug Administration.

T Staging

In patients with known bladder cancer, the important staging question is whether there is muscle invasion (stage T2 or higher) (Figs 4, 5, 9). The accuracy of contrast-enhanced CT in the local staging of bladder cancer is only 40%–60% (25,55). MR imaging is considered superior to CT in demonstrating the extent of bladder wall invasion (ie, in differentiating between stage T2a and stage T2b disease).

Microscopic perivesical spread (stage T3a disease) cannot be identified at either CT or MR imaging. Macroscopic perivesical disease (stage T3b) can be confidently diagnosed at CT only in the presence of moderate tumor volume outside the bladder. Perivesical fat stranding may often be seen following the treatment of bladder cancer due to surrounding edema or inflammation and does not necessarily signify stage T3b disease. Contrast-enhanced MR imaging is only moderately useful in differentiating stage T1 or lower tumors from stage T2 or higher tumors, with an accuracy of 75%–92% (36,40,56). The overall accuracy of contrast-enhanced MR imaging in determining tumor stage is 52%–93% (36,37,56–59).

Several recent studies have reported diffusion-weighted imaging to have a high sensitivity and specificity in the staging of bladder cancer

a.

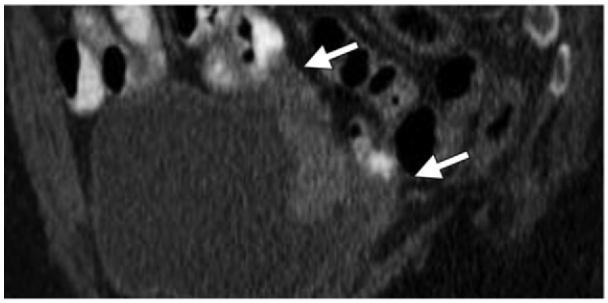

b.

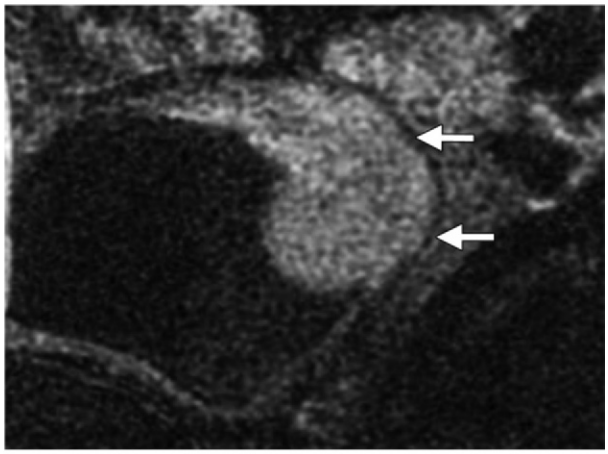

c.

Figure 11. Urothelial carcinoma (stage T2b) in a 62-year-old woman. **(a, b)** Axial **(a)** and sagittal **(b)** contrast-enhanced CT scans show an irregular 4.6-cm hyperattenuating mass at the posterosuperior bladder wall (arrows). There is a suggestion of small bowel involvement. **(c)** Sagittal diffusion-weighted image shows tumor extension into the bladder wall without perivesical involvement (arrows). Results of TURBT confirmed stage T2b disease.

(46,48–51). Takeuchi et al (50) reported an accuracy of 92% when a combination of three different MR imaging techniques (T2-weighted, contrast-enhanced, and diffusion-weighted imaging) were used to differentiate stage T1 tumors from stage T2 and higher disease. Diffusion-weighted imaging has the potential to complement other sequences in improving the diagnosis (Figs 10, 11) and staging of bladder cancer (38–42).

N Staging

The most common site of nodal metastasis is the obturator nodes. About one in six patients presents with lymph nodes above the aortic bifurcation, and 8% have presacral adenopathy (60). According to current TNM guidelines (Table), common iliac nodes are considered to be in a secondary drainage region and indicate stage N3 disease (according to previous TNM guidelines, they were considered to indicate distant metastases).

In lymph node staging, CT has an accuracy of 70%–90%, with false-negative rates of 25%–40%, whereas MR imaging has an accuracy of 64%–92% (53,61). Conventional CT and MR imaging cannot help identify metastases in lymph nodes less than 10 mm. Enlarged nodes may be reactive, so that specificity is also limited. Because extensive lymphadenectomy is increasingly being performed for muscle-invasive bladder cancer, there is less need for nodal staging of tumors in the pelvis. It is more important to identify nodes in the common iliac chain or in the retroperitoneum. According to recent published reports, diffusion-weighted imaging has shown promise in differentiating benign from malignant lymph nodes (Fig 12). Larger-scale studies will be required to determine the value of diffusion-weighted imaging in assessing early lymph node disease (62,63).

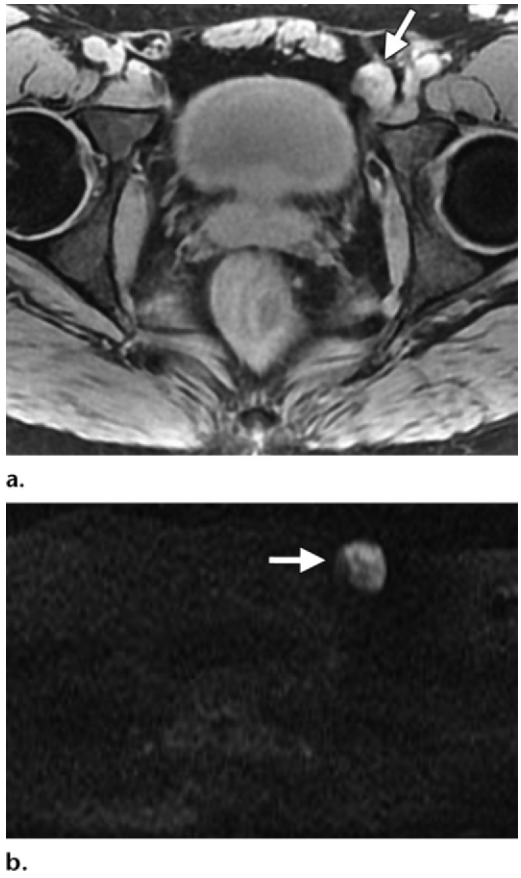

Figure 12. Metastatic urothelial carcinoma (micropapillary variant) in a 47-year-old man who had undergone TURBT 1 year earlier. **(a)** Axial fat-suppressed spoiled GRE image shows a left external iliac lymph node (arrow) with a maximum diameter of 1.5 cm. **(b)** On an axial diffusion-weighted image, the left external iliac lymph node (arrow) demonstrates high signal intensity and a low ADC value of 0.75 $\times 10^{-3}$ mm^2/sec, findings that are suggestive of malignancy. Bilateral lymphadenectomy helped confirm metastatic transitional cell carcinoma in the left external iliac lymph node chain.

Posttreatment Surveillance

Because of the high rate of local recurrence, patients with non-muscle-invasive bladder cancer must be followed up after treatment (Fig 13). Cystoscopy, urine cytology, and imaging of the upper tract with retrograde ureteroscopy are usually performed annually (24). Given the high metastatic recurrence rate of muscle-invasive bladder cancer, the National Comprehensive Cancer Network guidelines for postcystectomy surveillance include urine cytology, chest radiography, and abdominopelvic imaging every 3–6 months for the first 2 years. Following this period, imaging studies are indicated based on clinical status. Metastases usually occur in pelvic or retroperitoneal nodes. Less common sites of metastasis include the lungs, liver, adrenal glands, bones, and kidneys, and even the peritoneal space.

Conclusions

Early detection of bladder cancer is important, since up to 47% of bladder cancer–related deaths may have been avoided (64). Conventional CT and MR imaging are only moderately accurate in the diagnosis and local staging of bladder cancer; cystoscopy and pathologic staging remain the standards of reference. Whole-body CT is the primary imaging technique for detecting metastases in affected patients, especially those with muscle-invasive disease. The role of newer MR imaging sequences in the diagnosis and local staging of bladder cancer continues to evolve. Advances in MR imaging technology have made multiparametric MR imaging feasible for the local staging of bladder cancer to optimize treatment.

Acknowledgment.—The authors thank Ramya Wanigasooriya, MBBS, for her invaluable help in manuscript preparation.

Disclosures of Potential Conflicts of Interest.—**K.S.:** *Related financial activities:* none. *Other financial activities:* research grant from Siemens, consultant for Repligen.

References

1. Jemal A, Siegel R, Xu J, Ward E. Cancer statistics, 2010. CA Cancer J Clin 2010;60(5):277–300.
2. Avritscher EB, Cooksley CD, Grossman HB, et al. Clinical model of lifetime cost of treating bladder cancer and associated complications. Urology 2006; 68(3):549–553.
3. Yabroff KR, Lamont EB, Mariotto A, et al. Cost of care for elderly cancer patients in the United States. J Natl Cancer Inst 2008;100(9):630–641.
4. Skinner DG, Lieskovsky G, eds. Diagnosis and management of genitourinary cancer. Philadelphia, Pa: Saunders, 1988.
5. Murphy WM, Grignon DJ, Perlman EJ. Tumors of the kidney, bladder, and related urinary structures. AFIP Atlas of Tumor Pathology, ser 4. Washington, DC: American Registry of Pathology, 2004.
6. Kirkali Z, Chan T, Manoharan M, et al. Bladder cancer: epidemiology, staging and grading, and diagnosis. Urology 2005;66(6 suppl 1):4–34.
7. Murta-Nascimento C, Schmitz-Dräger BJ, Zeegers MP, et al. Epidemiology of urinary bladder cancer: from tumor development to patient's death. World J Urol 2007;25(3):285–295.

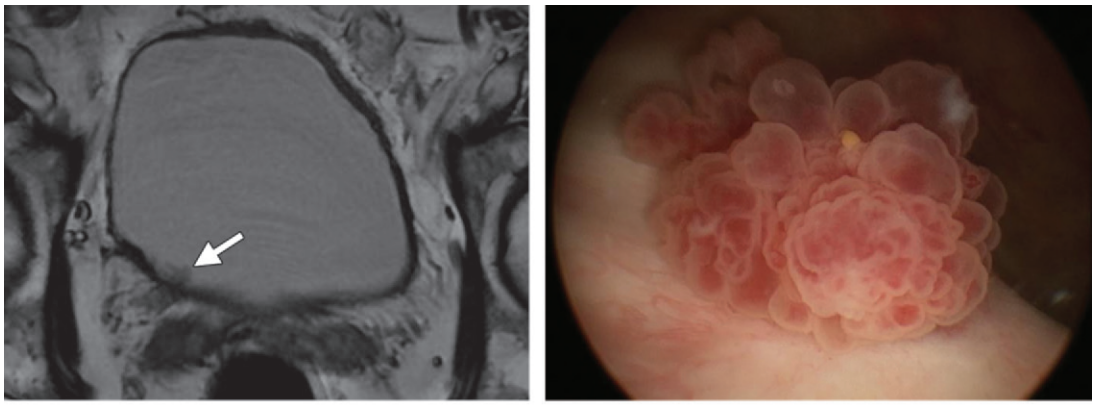

a. c.

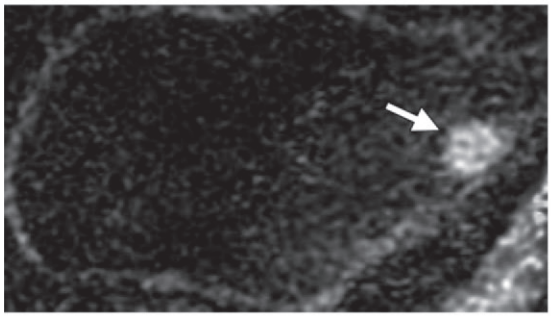

b.

Figure 13. Recurrent papillary urothelial carcinoma in a 74-year-old man who had undergone TURBT for stage Ta cancer 3 years earlier. **(a)** Axial T2-weighted MR image shows an 8-mm hypointense mass (arrow) at the right ureterovesical junction. The mass was not seen at initial flexible cystoscopy. **(b)** Sagittal diffusion-weighted image more clearly depicts the mass (arrow) at the right ureterovesical junction. **(c)** Follow-up cystoscopic image shows the ureterovesical junction mass.

8. Zeegers MP, Tan FE, Dorant E, van Den Brandt PA. The impact of characteristics of cigarette smoking on urinary tract cancer risk: a meta-analysis of epidemiologic studies. Cancer 2000;89(3):630–639.
9. Steiner H, Bergmeister M, Verdorfer I, et al. Early results of bladder-cancer screening in a high-risk population of heavy smokers. BJU Int 2008;102(3):291–296.
10. Aben KK, Witjes JA, Schoenberg MP, Hulsbergen-van de Kaa C, Verbeek AL, Kiemeney LA. Familial aggregation of urothelial cell carcinoma. Int J Cancer 2002;98(2):274–278.
11. Czene K, Lichtenstein P, Hemminki K. Environmental and heritable causes of cancer among 9.6 million individuals in the Swedish Family-Cancer Database. Int J Cancer 2002;99(2):260–266.
12. Saad A, Hanbury DC, McNicholas TA, Boustead GB, Morgan S, Woodman AC. A study comparing various noninvasive methods of detecting bladder cancer in urine. BJU Int 2002;89(4):369–373.
13. Sadow CA, Silverman SG, O'Leary MP, Signorovitch JE. Bladder cancer detection with CT urography in an academic medical center. Radiology 2008;249(1):195–202.
14. Pashos CL, Botteman MF, Laskin BL, Redaelli A. Bladder cancer: epidemiology, diagnosis, and management. Cancer Pract 2002;10(6):311–322.
15. Cote RJ, Dunn MD, Chatterjee SJ, et al. Elevated and absent pRb expression is associated with bladder cancer progression and has cooperative effects with p53. Cancer Res 1998;58(6):1090–1094.
16. Wu XR. Urothelial tumorigenesis: a tale of divergent pathways. Nat Rev Cancer 2005;5(9):713–725.
17. Shariat SF, Karakiewicz PI, Ashfaq R, et al. Multiple biomarkers improve prediction of bladder cancer recurrence and mortality in patients undergoing cystectomy. Cancer 2008;112(2):315–325.
18. Sexton WJ, Wiegand LR, Correa JJ, Politis C, Dickinson SI, Kang LC. Bladder cancer: a review of nonmuscle invasive disease. Cancer Contr 2010;17(4):256–268.
19. Wong-You-Cheong JJ, Woodward PJ, Manning MA, Sesterhenn IA. Neoplasms of the urinary bladder: radiologic-pathologic correlation. RadioGraphics 2006;26(2):553–580.
20. Greene FL, Page DL, Fleming ID, et al, eds. Urinary bladder. In: AJCC cancer staging manual. 6th ed. New York, NY: Springer-Verlag, 2002; 335–340.
21. Dutta SC, Smith JA Jr, Shappell SB, Coffey CS, Chang SS, Cookson MS. Clinical under staging of high risk nonmuscle invasive urothelial carcinoma treated with radical cystectomy. J Urol 2001;166(2):490–493.
22. Ficarra V, Dalpiaz O, Alrabi N, Novara G, Galfano A, Artibani W. Correlation between clinical and pathological staging in a series of radical cystectomies for bladder carcinoma. BJU Int 2005;95(6):786–790.
23. Herr HW. The value of a second transurethral resection in evaluating patients with bladder tumors. J Urol 1999;162(1):74–76.
24. Bradford TJ, Montie JE, Hafez KS. The role of imaging in the surveillance of urologic malignancies. Urol Clin North Am 2006;33(3):377–396.

25. Beyersdorff D, Zhang J, Schöder H, Bochner B, Hricak H. Bladder cancer: can imaging change patient management? Curr Opin Urol 2008;18(1):98–104.
26. Caterino M, Giunta S, Finocchi V, et al. Primary cancer of the urinary bladder: CT evaluation of the T parameter with different techniques. Abdom Imaging 2001;26(4):433–438.
27. Caoili EM, Cohan RH, Inampudi P, et al. MDCT urography of upper tract urothelial neoplasms. AJR Am J Roentgenol 2005;184(6):1873–1881.
28. Cowan NC, Turney BW, Taylor NJ, McCarthy CL, Crew JP. Multidetector computed tomography urography for diagnosing upper urinary tract urothelial tumour. BJU Int 2007;99(6):1363–1370.
29. Turney BW, Willatt JM, Nixon D, Crew JP, Cowan NC. Computed tomography urography for diagnosing bladder cancer. BJU Int 2006;98(2):345–348.
30. Knox MK, Cowan NC, Rivers-Bowerman MD, Turney BW. Evaluation of multidetector computed tomography urography and ultrasonography for diagnosing bladder cancer. Clin Radiol 2008;63(12):1317–1325.
31. Tsampoulas C, Tsili AC, Giannakis D, Alamanos Y, Sofikitis N, Efremidis SC. 16-MDCT cystoscopy in the evaluation of neoplasms of the urinary bladder. AJR Am J Roentgenol 2008;190(3):729–735.
32. Semelka RC. Abdominal-pelvic MRI. Hoboken, NJ: Wiley-Blackwell, 2010.
33. Lawler LP. MR imaging of the bladder. Radiol Clin North Am 2003;41(1):161–177.
34. Barentsz JO, Ruijs SH, Strijk SP. The role of MR imaging in carcinoma of the urinary bladder. AJR Am J Roentgenol 1993;160(5):937–947.
35. Hood MN, Ho VB, Smirniotopoulos JG, Szumowski J. Chemical shift: the artifact and clinical tool revisited. RadioGraphics 1999;19(2):357–371.
36. Tekes A, Kamel I, Imam K, et al. Dynamic MRI of bladder cancer: evaluation of staging accuracy. AJR Am J Roentgenol 2005;184(1):121–127.
37. Kim B, Semelka RC, Ascher SM, Chalpin DB, Carroll PR, Hricak H. Bladder tumor staging: comparison of contrast-enhanced CT, T1- and T2-weighted MR imaging, dynamic gadolinium-enhanced imaging, and late gadolinium-enhanced imaging. Radiology 1994;193(1):239–245.
38. Neuerburg JM, Bohndorf K, Sohn M, Teufl F, Guenther RW, Daus HJ. Urinary bladder neoplasms: evaluation with contrast-enhanced MR imaging. Radiology 1989;172(3):739–743.
39. Neuerburg JM, Bohndorf K, Sohn M, Teufl F, Günther RW. Staging of urinary bladder neoplasms with MR imaging: is Gd-DTPA helpful? J Comput Assist Tomogr 1991;15(5):780–786.
40. Hayashi N, Tochigi H, Shiraishi T, Takeda K, Kawamura J. A new staging criterion for bladder carcinoma using gadolinium-enhanced magnetic resonance imaging with an endorectal surface coil: a comparison with ultrasonography. BJU Int 2000;85(1):32–36.
41. Verma S, Rajesh A, Morales H, et al. Assessment of aggressiveness of prostate cancer: correlation of apparent diffusion coefficient with histologic grade after radical prostatectomy. AJR Am J Roentgenol 2011;196(2):374–381.
42. Hatano K, Tsuda K, Kawamura N, et al. Clinical value of diffusion-weighted magnetic resonance imaging for localization of prostate cancer: comparison with the step sections of radical prostatectomy [in Japanese]. Nippon Hinyokika Gakkai Zasshi 2010;101(4):603–608.
43. Kitajima K, Kaji Y, Fukabori Y, Yoshida K, Suganuma N, Sugimura K. Prostate cancer detection with 3 T MRI: comparison of diffusion-weighted imaging and dynamic contrast-enhanced MRI in combination with T2-weighted imaging. J Magn Reson Imaging 2010;31(3):625–631.
44. Kim CK, Park BK, Kim B. High-b-value diffusion-weighted imaging at 3 T to detect prostate cancer: comparisons between b values of 1,000 and 2,000 s/mm^2. AJR Am J Roentgenol 2010;194(1):W33–W37.

45. Sato C, Naganawa S, Nakamura T, et al. Differentiation of noncancerous tissue and cancer lesions by apparent diffusion coefficient values in transition and peripheral zones of the prostate. J Magn Reson Imaging 2005;21(3):258–262.
46. Matsuki M, Inada Y, Tatsugami F, Tanikake M, Narabayashi I, Katsuoka Y. Diffusion-weighted MR imaging for urinary bladder carcinoma: initial results. Eur Radiol 2007;17(1):201–204.
47. Koh DM, Takahara T, Imai Y, Collins DJ. Practical aspects of assessing tumors using clinical diffusion-weighted imaging in the body. Magn Reson Med Sci 2007;6(4):211–224.
48. Abou-El-Ghar ME, El-Assmy A, Refaie HF, El-Diasty T. Bladder cancer: diagnosis with diffusion-weighted MR imaging in patients with gross hematuria. Radiology 2009;251(2):415–421.
49. El-Assmy A, Abou-El-Ghar ME, Mosbah A, et al. Bladder tumour staging: comparison of diffusion- and T2-weighted MR imaging. Eur Radiol 2009;19 (7):1575–1581.
50. Takeuchi M, Sasaki S, Ito M, et al. Urinary bladder cancer: diffusion-weighted MR imaging—accuracy for diagnosing T stage and estimating histologic grade. Radiology 2009;251(1):112–121.
51. Watanabe H, Kanematsu M, Kondo H, et al. Preoperative T staging of urinary bladder cancer: does diffusion-weighted MRI have supplementary value? AJR Am J Roentgenol 2009;192(5):1361–1366.
52. Yoshida S, Koga F, Kawakami S, et al. Initial experience of diffusion-weighted magnetic resonance imaging to assess therapeutic response to induction chemoradiotherapy against muscle-invasive bladder cancer. Urology 2010;75(2):387–391.
53. Drieskens O, Oyen R, Van Poppel H, Vankan Y, Flamen P, Mortelmans L. FDG-PET for preoperative staging of bladder cancer. Eur J Nucl Med Mol Imaging 2005;32(12):1412–1417.
54. Kibel AS, Dehdashti F, Katz MD, et al. Prospective study of [18F]fluorodeoxyglucose positron emission tomography/computed tomography for staging of muscle-invasive bladder carcinoma. J Clin Oncol 2009;27(26):4314–4320.
55. Zhang J, Gerst S, Lefkowitz RA, Bach A. Imaging of bladder cancer. Radiol Clin North Am 2007;45(1): 183–205.
56. Narumi Y, Kadota T, Inoue E, et al. Bladder tumors: staging with gadolinium-enhanced oblique MR imaging. Radiology 1993;187(1):145–150.
57. Scattoni V, Da Pozzo LF, Colombo R, et al. Dynamic gadolinium-enhanced magnetic resonance imaging in staging of superficial bladder cancer. J Urol 1996; 155(5):1594–1599.
58. Barentsz JO, Jager G, Mugler JP 3rd, et al. Staging urinary bladder cancer: value of T1-weighted three-dimensional magnetization prepared-rapid gradient-echo and two-dimensional spin-echo sequences. AJR Am J Roentgenol 1995;164(1):109–115.
59. Tanimoto A, Yuasa Y, Imai Y, et al. Bladder tumor staging: comparison of conventional and gadolinium-enhanced dynamic MR imaging and CT. Radiology 1992;185(3):741–747.
60. Leissner J, Ghoneim MA, Abol-Enein H, et al. Extended radical lymphadenectomy in patients with urothelial bladder cancer: results of a prospective multicenter study. J Urol 2004;171(1):139–144.
61. Paik ML, Scolieri MJ, Brown SL, Spirnak JP, Resnick MI. Limitations of computerized tomography in staging invasive bladder cancer before radical cystectomy. J Urol 2000;163(6):1693–1696.
62. Ganeshalingam S, Koh DM. Nodal staging. Cancer Imaging 2009;9:104–111.
63. Mir N, Sohaib SA, Collins D, Koh DM. Fusion of high b-value diffusion-weighted and T2-weighted MR images improves identification of lymph nodes in the pelvis. J Med Imaging Radiat Oncol 2010;54 (4):358–364.
64. Morris DS, Weizer AZ, Ye Z, Dunn RL, Montie JE, Hollenbeck BK. Understanding bladder cancer death: tumor biology versus physician practice. Cancer 2009;115(5):1011–1020.

Urinary Bladder Cancer: Role of MR Imaging

Sadhna Verma, MD • Arumugam Rajesh, MBBS, FRCR • Srinivasa R. Prasad, MD • Krishnanath Gaitonde, MD • Chandana G. Lall, MD • Vladimir Mouraviev, MD, PhD • Gunjan Aeron, MD • Robert B. Bracken, MD • Kumaresan Sandrasegaran, MD

RadioGraphics 2012; 32:371–387 • **Published online** 10.1148/rg.322115125 • **Content Codes:** GU MR OI

Page 372
About 90% of bladder tumors are urothelial in origin (ie, transitional cell carcinomas).

Page 372
Urothelial tumors are classified as either invading muscle (nonpapillary) or not invading muscle (superficial or papillary).

Page 376
MR imaging has also been shown to better depict intramural tumor invasion as well as extravesical extension and allows differentiation between muscle-invasive and non-muscle-invasive disease.

Page 377
High-resolution fast SE T2-weighted images of the bladder obtained in the three orthogonal planes with a small FOV and a large matrix are used to evaluate the detrusor muscle for tumor depth and invasion of the surrounding organs (36).

Page 380 (Figure 3 on page 376. Figure 4 on page 377. Figure 8 on page 380)
The bladder tumor, mucosa, and submucosa enhance early, but the muscle layer maintains its hypointensity and enhances late (60 sec) (Figs 3, 4, 8) (36).